SCIENTIFIC REPORTS

OPEN

SUBJECT AREAS:
METALS AND ALLOYS
NANOWIRES
STRUCTURAL PROPERTIES
COMPOSITES

Received
30 July 2014

Accepted
3 October 2014

Published
24 October 2014

Correspondence and requests for materials should be addressed to L.C. (lishancui63@126.com) or Y.L. (yinong.liu@uwa.edu.au)

Locality and rapidity of the ultra-large elastic deformation of Nb nanowires in a NiTi phase-transforming matrix

Shan Wang[1], Lishan Cui[1], Shijie Hao[1], Daqiang Jiang[1,2], Yinong Liu[2], Zhenyang Liu[1], Shengcheng Mao[3], Xiaodong Han[3] & Yang Ren[4]

[1]State Key Laboratory of Heavy Oil Processing and Department of Materials Science and Engineering, China University of Petroleum, Beijing 102249, China, [2]School of Mechanical and Chemical Engineering, The University of Western Australia, Crawley, WA 6009, Australia, [3]Institute of Microstructure and Properties of Advanced Materials, Beijing University of Technology, Beijing 100124, China, [4]X-ray Science Division, Argonne National Laboratory, Argonne, Illinois 60439, USA.

This study investigated the elastic deformation behaviour of Nb nanowires embedded in a NiTi matrix. The Nb nanowires exhibited an ultra-large elastic deformation, which is found to be dictated by the martensitic transformation of the NiTi matrix, thus exhibiting unique characteristics of locality and rapidity. These are in clear contrast to our conventional observation of elastic deformations of crystalline solids, which is a homogeneous lattice distortion with a strain rate controlled by the applied strain. The Nb nanowires are also found to exhibit elastic-plastic deformation accompanying the martensitic transformation of the NiTi matrix in the case when the transformation strain of the matrix over-matches the elastic strain limit of the nanowires, or exhibit only elastic deformation in the case of under-matching. Such insight provides an important opportunity for elastic strain engineering and composite design.

One research that has received very keen interest recently is elastic strain engineering[1–6], in which new and extraordinary functional properties of solids, such as magnetic, photonic, electronic, superconducting and catalytic property can be explored by inducing large elastic strains to alter the electronic state of a solid. Recently, much effort has been given to explore ultra-large elastic strains in solids[1,7–13]. However, most approaches are only applicable at microscales[7–11] or in micro regions[12,13], which hardly have any macroscopic effects for meaningful applications. It is a challenge to achieve ultra-large elastic strains in solids in large quantity at macroscopic scale. One promising strategy is to use a unique composite system consisting of nanowires and martensitic phase-transforming matrix[14].

Such composite system imposes a unique mechanics condition for the elastic nanowires embedded in a matrix that deforms by a different mechanism of martensitic transformation. It is known that the ultra-large elastic deformation[7,10–12] of nanowires proceeding via lattice expansion is homogenous in nature. The strain rate of elastic deformation is also in response to and controlled by the external stimulus (e.g., applied strain). In contrast, the martensitic transformation deformation[15,16], in the context of lattice distortion, presents a very different process. Being a first order transformation of diffusionless lattice distortion, the martensitic transformation exhibits a discrete and inhomogeneous lattice strain field between its parent phase and the martensite phase, giving the transformation its locality nature. In addition, as a cooperative atomic shuffling process, the transformation proceeds at the speed of mechanical shock wave (i.e., speed of sound) in the solid, giving it its rapidity nature, irrespective of the rate of the applied strain. Then the question is that, given that the components in the composite system deform in contrasting deformation mechanisms at the crystal lattice scale (as summarized in Table 1), how will the characteristics of the ultra-large elastic deformation of the nanowires be influenced by the martensitic transformation of the matrix?

In this study, we designed an in-situ Nb nanowire - NiTi matrix composite fabricated by means of ingot casting and wire drawing. The matrix in this composite transforms in a macroscopically inhomogeneous Lüders-like manner[17–19], which provides an opportunity to observe the lattice strain interactions between the embedded nanowires and the NiTi matrix at macro-scale during deformation by using HE-XRD method. This communication reports the main findings of this study.

Table 1 | Contrasting characteristics of the elastic deformation of nanowires and martensitic transformation deformation of the matrix

	Lattice strain	Lattice strain rate
Elastic deformation	Homogeneous	Progressive and controlled by applied strain rate
Martensitic transformation deformation	Inhomogeneous and discrete (Locality)	Speed of sound and irrespective of applied strain rate (Rapidity)

Results

Figure 1 shows microstructural analysis of the composite wire. Transmission electron microscopic (TEM) examination (Figure 1a) and back scattered scanning electron micrograph (BSEM) (the inset) reveal that the composite consists of Nb nanowires well dispersed and well aligned in the NiTi matrix along the wire axial direction. The ribbon-shaped Nb nanowires are 5 ~ 20 nm in thickness, 20 ~ 200 nm in width and are in various lengths ranging from hundreds of nanometers to longer than 1 μm. The 2D HE-XRD pattern (Figure 1b) indicates that the composite contains body-centered cubic Nb and B2–NiTi phases, and the Nb nanowires have almost an exclusive [110] orientation along the axial direction of the composite wire.

In-situ HE-XRD was carried out on the composite wire during tensile deformation cycles. The stress-strain curve of the composite wire (Figure 2a) exhibits a pseudoelastic behaviour in typical Lüders-like transformation manner with a stress plateau[17–19]. Figure 2b displays the evolution of diffraction peaks for planes perpendicular to the loading direction during the first loading process. It is seen that during the initial apparent elastic deformation of the composite in stage O→A, the B2-NiTi (211) diffraction peak shifted progressively to higher d-spacing values, as expected under tensile deformation. During stress-induced martensitic transformation in stage A→B, position of the B2–NiTi (211) diffraction peak remained constant. With continuous deformation from B to C, the B2-NiTi (211) peak abruptly disappeared and the B19'-NiTi (001) peak appeared. This observation indicates that the B2→B19' martensitic transformation in the NiTi matrix did not occur at the X-ray observation point until stage B→C, demonstrating the Lüders-like transformation behaviour[17–19].

Figure 2c displays the evolution of the lattice strain with respect to the applied strain for Nb (220) planes perpendicular to the loading direction during the first deformation cycle. It is seen that during deformation, the lattice strain of the Nb nanowires increased practically linearly with the applied strain in the initial elastic stage (O→A). After that, the elastic strain of the Nb nanowires remained constant (A→B), as the B2→B19' transformation occurred elsewhere away from the X-ray observation point. In stage B→C, the elastic strain of the Nb nanowires showed a sudden increase from 1.4% to 5.2%. This sudden change coincides with the disappearance

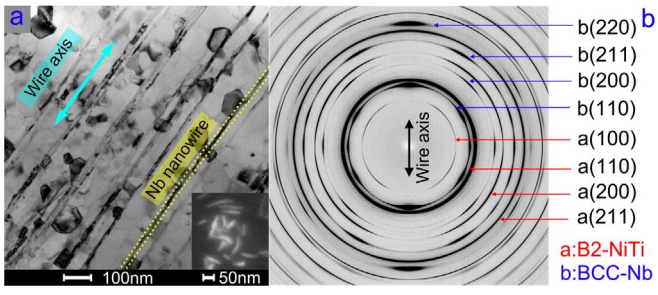

Figure 1 | Typical microstructure of the nanowire composite. (a) TEM bright field image and BSEM image illustrating the longitudinal section and cross section (inset: bright regions, cross sections of Nb nanowires; dark regions, NiTi matrix) view of the composite. (b) 2D HE-XRD pattern of the composite wire.

of the B2-NiTi (211) diffraction peak and the appearance of the B19'-NiTi (001) peak (Figure 2b), implying the arrival of the front of the Lüders band of the B2→B19' transformation at the X-ray observation point. The increment of elastic strain of the Nb nanowires (3.8%) is ~13 times more than that of the applied strain (0.3%) over the same period. This explicitly demonstrates that the occurrence of the ultra-large elastic strain of the Nb nanowires during tensile deformation is dictated by the stress-induced martensitic transformation of the NiTi matrix, instead of the applied strain.

Figure 2d shows the evolution of diffraction peaks for planes perpendicular to the loading direction during the pseudoelastic recovery process upon unloading, and Figure 2c shows the corresponding evolution of the elastic strain of the Nb nanowires. It is seen that with decreasing the applied strain, after the initial elastic recovery of the Nb nanowires and NiTi matrix (D→E), the elastic strain of the Nb nanowires experienced a sudden drop from 3.1% to −0.7% (F→G), apparently associated with the reverse martensitic transformation of NiTi matrix. This is confirmed by the appearance of the B2-NiTi (211) diffraction peak and disappearance of the B19'-NiTi (001) diffraction peak in stage F→G, as evident in Figure 2d. The decrement of elastic strain of the Nb nanowires (3.8%) is ~13 times more than that of the applied strain (0.3%) during the same period. This demonstrates that the ultra-large elastic recovery deformation of Nb nanowires during unloading is also dictated by the reverse martensitic transformation of the NiTi matrix.

These observations upon loading and unloading explicitly demonstrate that the ultra-large elastic deformation of the Nb nanowires is dictated by and synchronized with the martensitic transformation of the NiTi matrix. Because that the martensitic transformation proceeds with locality and rapidity, the ultra-large elastic deformation of the Nb nanowires in the phase-transforming NiTi matrix also exhibits these two characteristics, which is quite different from the elastic deformation behaviour of free standing nanowires.

Based on the above discussion, it is clear that during the martensitic transformation of the NiTi matrix, the local magnitude of deformation of the embedded Nb nanowires is dictated by the magnitude of transformation strain of the matrix, irrespective of the magnitude of the applied macroscopic strain. Following this, it can be expected that, in the case that the magnitude of the transformation strain over-matches the elastic strain limit of the nanowires, the embedded nanowires will exhibit elastic-plastic deformation during the lattice distortion of the martensitic transformation of the matrix. On the other hand, when the transformation strain just matches or under-matches the elastic strain limit of the nanowires, the embedded nanowires will exhibit pure elastic deformation during the process of transformation. This is in fact evident in the following analysis. It is noted that a compressive residual strain of −1.3% was generated in the Nb nanowires at the end of the first deformation cycle (point H in Figure 2c). This is caused by the fact that the elastic strain limit of the Nb nanowires were not large enough to match with the transformation strain of the matrix, and the Nb nanowires were forced to elongate to beyond their elastic limit into plastic deformation during the lattice distortion of martensitic transformation of the NiTi matrix. The plastically deformed Nb nanowires were consequently subjected to compression when the NiTi matix underwent the reverse transformation to recover its original length upon unloading. This depicts a situation of over-matching of the matrix transformation strain to the elastic strain limit of the nanowires.

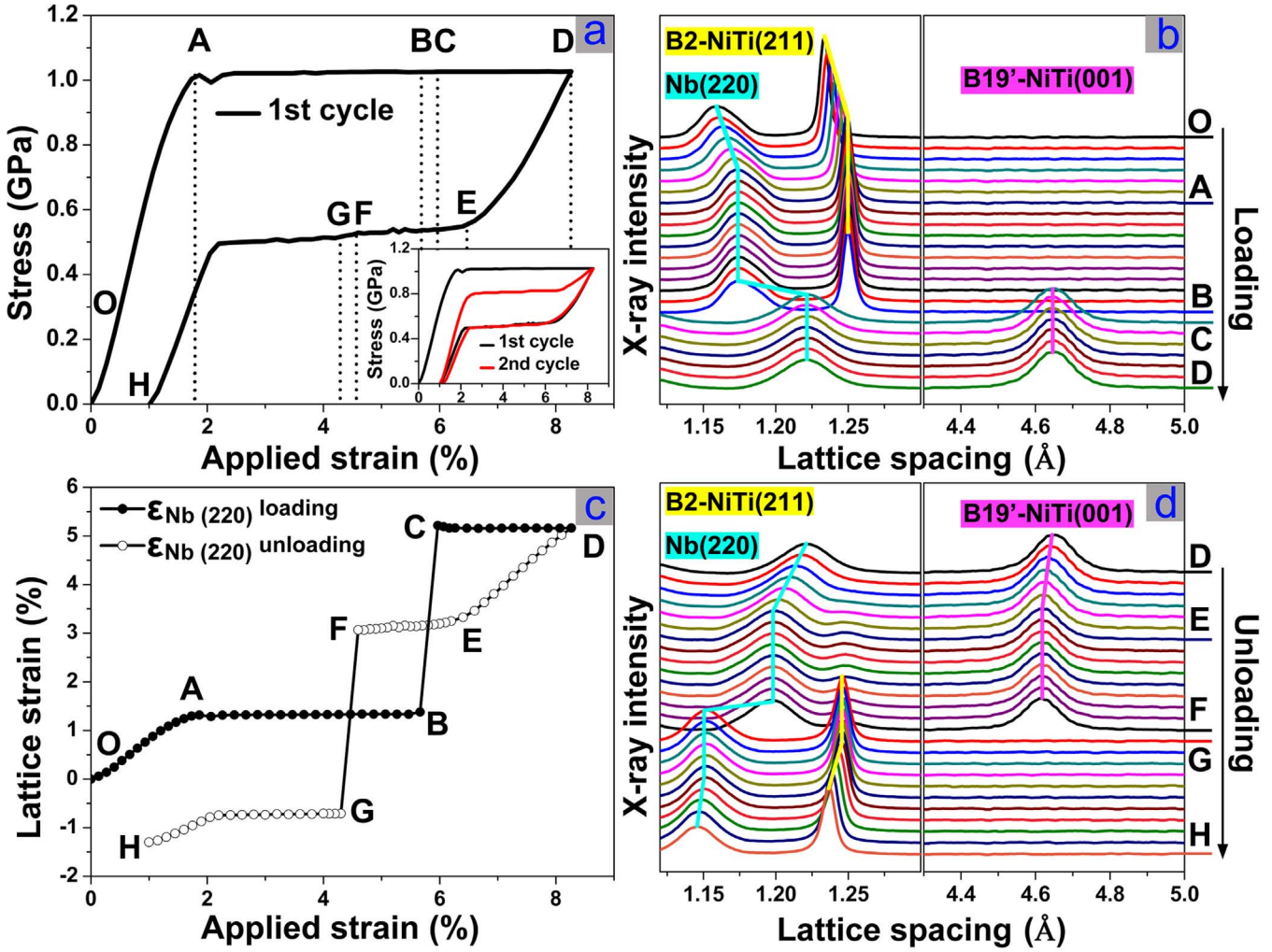

Figure 2 | Synchronization of the ultra-large elastic deformation of Nb nanowires and the martensitic phase transformation of NiTi matrix. (a) Macroscopic tensile stress-strain curve during the first and the whole (inset) cycling. (b) Evolution of the diffraction peaks for Nb (220), B2–NiTi (211) and B19'–NiTi (001) planes perpendicular to the loading direction during loading. (c) Evolution of the lattice strain with respect to the applied strain for Nb (220) plane perpendicular to the loading direction during the first cycle. (d) Evolution of the diffraction peaks for Nb (220), B2–NiTi (211) and B19'–NiTi (001) planes perpendicular to the loading direction during unloading.

Figure 3 displays the deformation behaviour of the Nb nanowires in the second deformation cycle. It is seen that the Nb nanowires exhibited an increased elastic strain range of 6.4% (O→D). This is apparently due to the pre-existing compressive strain of −1.3% formed at the end of the first cycle (point O in Figure 3a), adding to the tensile strain of 5.1%. It is also evident that the Nb nanowires experienced further elastic deformation (C→D) after the sudden increase in elastic strain associated with the martensitic transformation (A→B). This further elastic deformation is accompanied by the elastic deformation of B19'-NiTi (red box), and is apparently benefiting from the increased elastic strain range of the nanowires. This implies that the elastic strain limit of the Nb nanowires is large enough to match with the transformation strain of the matrix and also some elastic strain of the martensite. In this case, nearly no plastic deformation occurred in the Nb nanowires during the lattice distortion of the martensitic transformation, as indicated by the fact that the elastic strain of the Nb nanowires returned to the original value (point O) after unloading. This represents the situation of under-matching of the transformation strain of the matrix to the elastic strain limit of the nanowires.

In this study, we demonstrated that the ultra-large elastic deformation of the Nb nanowires embedded in a NiTi matrix is dictated by and synchronized with the stress-induced martensitic transformation of the matrix, exhibiting the characteristics of locality and rapidity. Given that the local strain of the Nb nanowires is dictated by the martensitic lattice distortion of the NiTi matrix, the nanowires exhibit both ultra-large elastic deformation and plastic deformation during the lattice distortion of the martensitic transformation of the matrix in the case when the lattice strain of the martensite over-matches the elastic strain limit of the nanowires, or experience only ultra-large elastic deformation in the case of strain under-matching. This communication reveals the distinct characteristics of elastic deformation of nanowires in martensitic phase-transforming matrices, which has implications for the development of elastic strain engineering and composite design.

Methods

An ingot with a composition of $Ti_{44}Ni_{47}Nb_9$ (at.%) was prepared by means of vacuum induction melting. The ingot was hot forged at 850°C into a bar of 16 mm in diameter, and hot drawn into a thin wire of 0.5 mm in diameter. The wire was then annealed at 500°C for 20 min followed by air cooling. The microstructure of the wire was analyzed using a FEI F20 transmission electron microscope operated at 200 kV and a FEI Quanta 200F scanning electron microscope operated at 20 kV.

In situ synchrotron HE-XRD experiments were performed at beamline 11-ID-C of the Advanced Photon Source at Argonne National Laboratory. The beamline was used in the Debye–Scherrer transmission geometry, with a monochromatic beam of 0.108 Å wavelength and 0.8 × 0.8 mm in size. The X-ray diffraction patterns were collected at a fixed position within the gauge length during tensile deformation. In-

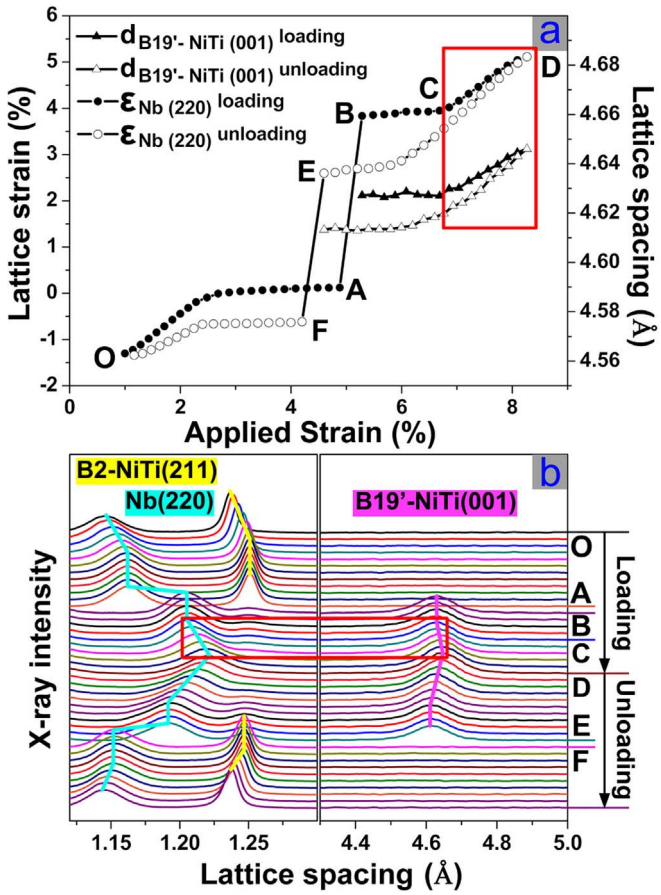

Figure 3 | Ultra-large elastic deformation of Nb nanowires accompanied by the martensitic phase transformation of the NiTi matrix during the second cycle. (a) Evolution of the lattice strain and lattice spacing with respect to the applied strain respectively for Nb (220) and B19'–NiTi(001) planes perpendicular to the loading direction during the second cycle. (b) Evolution of the diffraction peaks for Nb (220), B2–NiTi (211) and B19'–NiTi (001) planes perpendicular to the loading direction during the second cycle.

situ tensile test was performed using an Instron testing machine at room temperature at a strain rate of $1 \times 10^{-4}s^{-1}$. The sample had a gauge length of 25 mm. The lattice strain is determined as $(d_{hkl}-d_{hkl}^{0})/d_{hkl}^{0}$, in which d_{hkl}^{0} is the peak position at zero applied stress. Gaussian fits were used to determine peak positions. Errors of the d-spacing strain measurement are estimated to be smaller than 0.1%.

1. Zhu, T. & Li, J. Ultra-strength materials. *Prog. Mater. Sci.* **55**, 710–757 (2010).
2. Levy, N. *et al.* Strain-induced pseudo–magnetic fields greater than 300 tesla in graphene nanobubbles. *Science* **329**, 544–547 (2010).
3. Signorello, G. *et al.* Inducing a direct-to-pseudodirect bandgap transition in wurtzite GaAs nanowires with uniaxial stress. *Nat. Commun.* **5**, 3655 (2014).
4. Cao, J. *et al.* Strain engineering and one-dimensional organization of metal-insulator domains in single-crystal vanadium dioxide beams. *Nat. Nanotech.* **4**, 732–737 (2009).
5. Locquet, J.-P. *et al.* Doubling the critical temperature of $La_{1.9}Sr_{0.1}CuO_4$ using epitaxial strain. *Nature* **394**, 453–456 (1998).
6. Strasser, P. *et al.* Lattice-strain control of the activity in dealloyed core-shell fuel cell catalysts. *Nat. Chem.* **2**, 454–460 (2010).
7. Wei, B. *et al.* Size-dependent bandgap modulation of ZnO nanowires by tensile strain. *Nano Lett.* **12**, 4595–4599 (2012).
8. Wang, Y. *et al.* Super deformability and Young's modulus of GaAs nanowires. *Adv. Mater.* **23**, 1356–1360 (2011).
9. Tian, L. *et al.* Approaching the ideal elastic limit of metallic glasses. *Nat. Commun.* **3**, 609 (2012).
10. Richter, G. *et al.* Ultrahigh strength single crystalline nanowhiskers grown by physical vapor deposition. *Nano Lett.* **9**, 3048–3052 (2009).
11. Zhu, Y. *et al.* Mechanical properties of vapor-liquid-solid synthesized silicon nanowires. *Nano Lett.* **9**, 3934–3939 (2009).
12. Yue, Y., Liu, P., Zhang, Z., Han, X. & Ma, E. Approaching the theoretical elastic strain limit in copper nanowires. *Nano Lett.* **11**,3151–3155 (2011).
13. Rodrigues, V. & Ugarte, D. Real-time imaging of atomistic process in one-atom-thick metal junctions. *Phys. Rev. B* **63**,073405 (2001).
14. Hao, S. J. *et al.* A transforming metal nanocomposite with large elastic strain, low modulus and high strength. *Science* **339**, 1191–1194 (2013).
15. Nishiyama, Z. *Martensitic Transformations.* (Academic Press, New York 1978).
16. Patoor, E. *et al.* Shape memory alloys, Part I: General properties and modeling of single crystals. *Mech. Mater.* **38**, 391–429 (2006).
17. Sittner, P., Liu, Y. & Novak, V. On the origin of Lüders-like deformation of NiTi shape memory alloys. *J. Mech. Phys. Solids.* **53**, 1719–1746 (2005).
18. Shaw, J. A. & Kyriakides, S. Acta Mater. On the nucleation and propagation of phase transformation fronts in a NiTi alloy. *Acta Mater.* **45**, 683–700 (1997).
19. Young, M. L., Wagner, M. F.-X., Frenzel, J., Schmahl, W. W. & Eggeler, G. Phase volume fractions and strain measurements in an ultrafine-grained NiTi shape-memory alloy during tensile loading. *Acta Mater.* **58**, 2344–2354 (2010).

Acknowledgments

This work is supported by the National Natural Science Foundation of China (NSFC) (11474362), the key program project of NSFC (51231008), the National 973 programs of China (2012CB619403), Australian Research Council (DP140103805) and the Key Project of Chinese Ministry of Education (313055). Use of the Advanced Photon Source was supported by the U.S. Department of Energy, Office of Science, under contract no. DE-AC02-06CH11357.

Author contributions

L.C. and Y.L. designed the project. S.W. carried out materials preparation and testing. S.W., Z.L. and S.M. carried out the SEM and TEM experiments. X.H. and D.J. supervised the TEM experiments. S.H. carried out the synchrotron experiments. Y.R. supervised the synchrotron experiments. S.W., L.C. and Y.L. wrote the initial drafts and final version of the manuscript.

Additional information

Competing financial interests: The authors declare no competing financial interests.

How to cite this article: Wang, S. *et al.* Locality and rapidity of the ultra-large elastic deformation of Nb nanowires in a NiTi phase-transforming matrix. *Sci. Rep.* **4**, 6753; DOI:10.1038/srep06753 (2014).